

Quantum Critical Magnetic Excitations in Spin-1/2 and Spin-1 Chain Systems

L. S. Wang,¹ Y. Xu,^{2,*} Y. Y. Huang,¹ J. M. Ni,¹ C. C. Zhao,¹ Y. F. Dai,¹ B. Y. Pan,^{1,3}
X. C. Hong,¹ P. Chauhan,⁴ S. M. Koochpayeh,^{4,5} N. P. Armitage,⁴ and S. Y. Li^{1,6,7,†}

¹*State Key Laboratory of Surface Physics, and Department of Physics, Fudan University, Shanghai 200438, China*

²*Key Laboratory of Polar Materials and Devices (MOE),*

School of Physics and Electronic Science, East China Normal University, Shanghai 200241, China

³*School of Physics and Optoelectronic Engineering,*

Ludong University, Yantai, Shandong 264025, China

⁴*The Institute for Quantum Matter, Department of Physics and Astronomy,
The Johns Hopkins University, Baltimore, Maryland 21218, USA*

⁵*Department of Materials Science and Engineering,*

The Johns Hopkins University, Baltimore, Maryland 21218, USA

⁶*Collaborative Innovation Center of Advanced Microstructures, Nanjing 210093, China*

⁷*Shanghai Research Center for Quantum Sciences, Shanghai, 201315, China*

(Dated: December 6, 2021)

The study of CoNb_2O_6 sits at the confluence of simplicity and complexity: on one hand, the model for Ising chains—the building blocks of CoNb_2O_6 —in a transverse field, can be exactly solved and, thus, serves as an archetype of quantum criticality; on the other hand, the weak but nonzero interchain coupling adds geometric frustration to the stage, substantially complicating the phase diagram. Here we utilize low-temperature specific heat and thermal conductivity measurements to study the low-lying magnetic excitations in CoNb_2O_6 and its spin-1 analogue NiNb_2O_6 . The thermal conductivity is found to be suppressed around the quantum critical point, where the specific heat is enhanced due to gapless magnetic excitations, pointing to the localized nature of the latter. These results highlight the predominant role of frustration in determining the quantum critical magnetic excitations of spin chains, which may furthermore underlie the remarkable similarities between the phenomenology of these spin-1/2 and spin-1 systems.

I. INTRODUCTION

Quantum aspects are particularly evident in low-dimensional systems, leading to substantial corrections to classical pictures. In the context of magnetism, excitations with fractionalized quantum number (e.g., spinons) [1, 2] and the Haldane phase [3, 4] are among the most well-known examples. Under specific circumstances, the low dimensionality can lead to simplification. For instance, by mapping to a spinless fermion system, the transverse-field Ising chain (TFIC) model can be exactly solved [5, 6]. The closest realization of this model has long been thought to be CoNb_2O_6 under a transverse field [7–17].

The physics of CoNb_2O_6 , however, extends far beyond: when isolated, the spin-1/2 Ising chains, as the building blocks, order ferromagnetically only at zero temperature, and its evolution under a transverse field can be described elegantly by the TFIC model, featuring a transition to paramagnetic state at an one-dimensional (1D) quantum critical point (QCP) [18]; on the flip side, CoNb_2O_6 being quasi-1D means that these Ising chains are weakly coupled to give rise to 3D magnetic phases at finite temperatures, which terminate at a 3D QCP slightly above the 1D one [11, 19, 20]. The arrangement of the Ising chains on a triangular lattice brings in geometric frus-

tration, which is notoriously challenging to tackle [21]. Such a Janus-faced nature of CoNb_2O_6 has led to several beautiful demonstrations: while subtle properties of 1D Ising quantum critical physics were unveiled by spectroscopy [7, 10, 12–14, 16, 17, 22], a plethora of magnetic phases were theoretically predicted as a result of the interplay between quantum criticality and frustration [9]. Moreover, it was shown recently that the frustration-induced quantum motion of domain walls can be described by a model of twisted Kitaev chain, reminiscent of the honeycomb Kitaev spin liquid [17].

Central to these studies is the detection of the magnetic excitations across the QCP [10–16, 23]. In low-energy probes like nuclear magnetic resonance, the quasielastic mode associated with domain-wall quasiparticles (kinks) was found to disappear above the 1D QCP [11]. Neutrons create pairs of kinks in the ordered phase, which were observed to change character to spin-flips in the paramagnetic phase [10]. Most prominently, around the 1D QCP, discrete modes were observed both by neutron and time-domain terahertz (THz) spectroscopy, with the energy ratio of the two lowest-lying ones approaching the golden mean predicted for the E8 spectrum, which E8 referring to the maximum exceptional Lie algebra [7, 10, 14, 16]. In this context, the bound pairs of kinks can be viewed as the solid-state version of mesons composed of a quark and an antiquark [7]. Specific heat study revealed a significant band of gapless fermionic magnetic excitations around the 3D QCP, constituting a large portion of the total spin density of states [15]. These gapless excita-

* yxu@phy.ecnu.edu.cn

† shiyuan.li@fudan.edu.cn

tions were argued to be distinct from the discrete modes evident in spectroscopy [15]. The comprehensive understanding of the magnetic excitations around the QCPs in CoNb_2O_6 out of the results from various probes remains to be understood.

Low-temperature thermal conductivity measurement has proven to be a powerful means in the study of magnetic excitations in low-dimensional magnets [24–45]. Here, we utilize such measurements down to 60 mK to investigate the quantum critical magnetic excitations in CoNb_2O_6 . We observed an absence of direct contribution to the thermal conductivity from the gapless fermionic magnetic excitations evident in specific heat around the QCP. Furthermore, the thermal conductivity was found to be diminished in the field range where specific heat is enhanced. These results are interpreted as the scattering of heat-carrying phonons off localized magnetic excitations around the QCP, signalling a prominent role of frustration in determining these quantum critical magnetic excitations. A similar set of phenomenology was also observed in the quasi-1D spin-1 Heisenberg ferromagnetic chain system NiNb_2O_6 . The similarity between the two compounds is remarkable, considering the apparently distinct settings of spin quantum number, patterns of long-range order, and magnetic anisotropy.

II. METHODS

As illustrated in Fig. 1(a), both columbite CoNb_2O_6 and NiNb_2O_6 crystallize in the space group $Pbcn$, consisting of zigzag chains of edge-sharing octahedra along the crystallographic c axis with ferromagnetic interactions between nearest-neighbor effective spin-1/2 Co^{2+} or spin-1 Ni^{2+} ions, respectively, and the interchain coupling is considerably smaller [46, 47]. In CoNb_2O_6 , a strong single-ion anisotropy due to crystal field effects from the distorted CoO_6 octahedra forces the Co^{2+} spins to be Ising aligned along the local easy axis, which lies canted from the ac plane in an alternating fashion from bond to bond and slightly cants away from the c axis [17, 46, 48–50]. In the ab plane, the weakly coupled Ising chains sit on a triangular lattice, a prototypical motif for geometric frustration [21]. The magnetism in NiNb_2O_6 is more isotropic, so that the exchange coupling can be described by a Heisenberg term, with an additional term for the uniaxial anisotropy [51, 52]. Frustration has also been argued to manifest itself in NiNb_2O_6 [51].

Single crystals of CoNb_2O_6 and NiNb_2O_6 were grown at Fudan University and the Johns Hopkins University, respectively, by the floating zone method and oriented by Laue diffraction. The specific heat of NiNb_2O_6 was measured by the relaxation method in a Quantum Design physical property measurement system equipped with a dilution refrigerator. For the thermal conductivity measurements, the CoNb_2O_6 and NiNb_2O_6 samples were cut into a rectangular shape of dimensions $2.0 \times 0.5 \times 0.5$

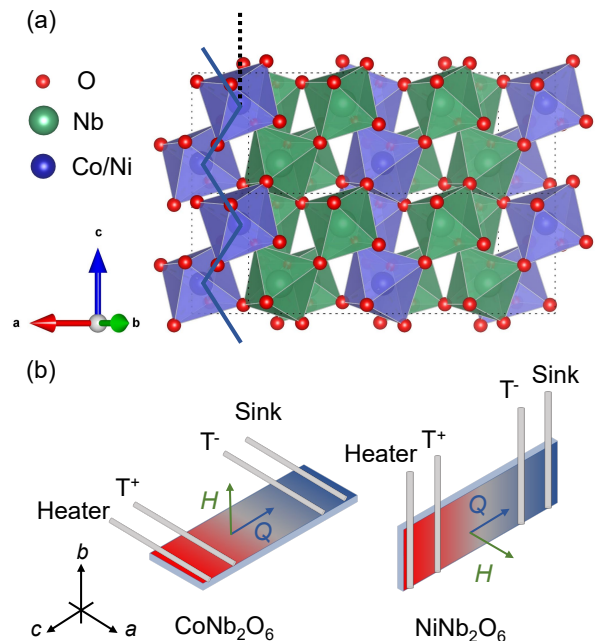


FIG. 1. (a) The crystal structure of CoNb_2O_6 and NiNb_2O_6 . The blue solid line highlights the zigzag chain formed by Co/Ni spins. Note the finite canting angle between the local easy axis and the c axis, with the latter shown by the thick dotted line and the direction of the former not to be confused with the zigzag chain. (b) The experimental setup for thermal conductivity measurements for CoNb_2O_6 and NiNb_2O_6 . The magnetic field was applied along b for CoNb_2O_6 and along a for NiNb_2O_6 .

mm^3 and $2.1 \times 0.3 \times 0.1 \text{ mm}^3$, respectively, with the longest dimension along the c axis. Four silver wires were attached to the sample with silver paint for thermal conductivity measurements with a heat current along c . The thermal conductivity was measured in a dilution refrigerator, using a standard four-wire steady-state method with two RuO_2 chip thermometers, calibrated *in situ* against a reference RuO_2 thermometer. Figure 1(b) gives a schematic of the experimental setup for thermal conductivity measurements, with a heat current along the chain direction c and transverse magnetic fields along b for CoNb_2O_6 and along a for NiNb_2O_6 , respectively. The specific heat of NiNb_2O_6 was also measured with the magnetic field along the a axis.

III. RESULTS AND DISCUSSIONS

A. Magnetic excitations around the QCP in CoNb_2O_6

The specific heat C data extracted from Ref. [15] and our thermal conductivity κ data for CoNb_2O_6 are compiled in Fig. 2. As shown in Fig. 2(a), the 3D magnetic

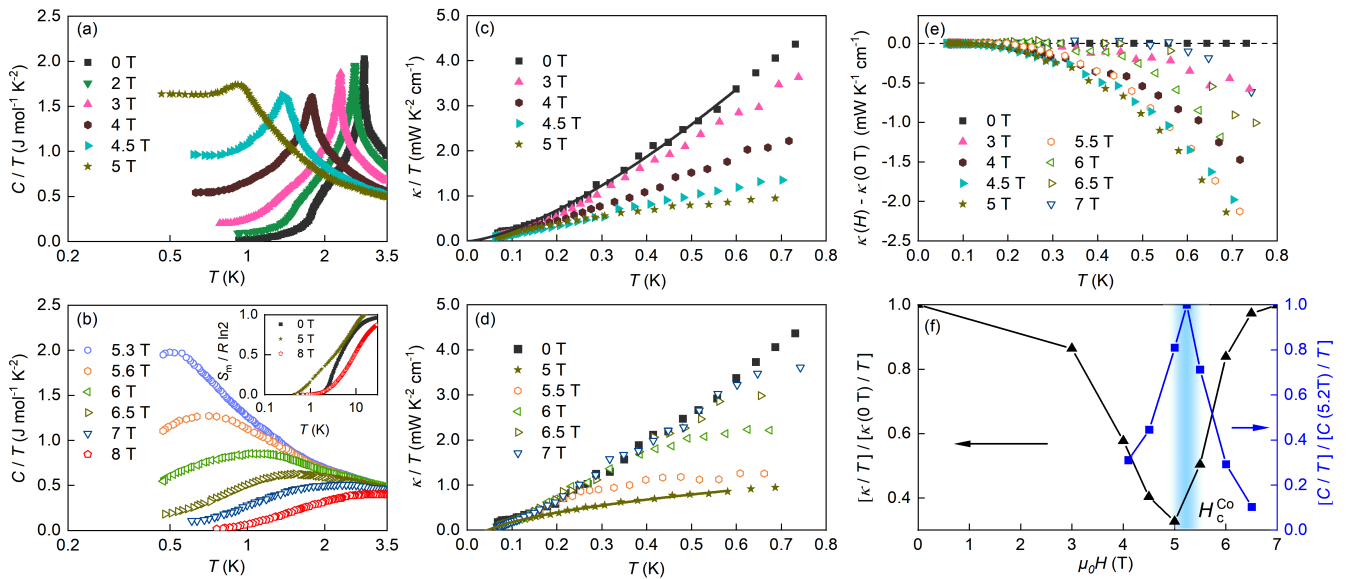


FIG. 2. (a,b) The specific heat C/T of CoNb_2O_6 below and above $\mu_0 H_c^{\text{Co}} \sim 5.24$ T, respectively. The inset of (b) shows the magnetic entropy S_m of CoNb_2O_6 at selected fields. The data in these two panels were adapted from Ref. [15]. (c,d) The thermal conductivity κ/T of CoNb_2O_6 at fields below and above H_c^{Co} , respectively. The solid lines are the fitting of the 0 and 5 T data to $\kappa/T = a + bT^{\alpha-1}$. (e) The influence of magnetic excitations on the thermal conductivity reflected in $\Delta\kappa \equiv \kappa(H) - \kappa(0 \text{ T})$. (f) The magnetic field evolution of the normalized thermal conductivity and magnetic specific heat at 0.45 K. The cyan shaded region depicts the position of H_c^{Co} .

order onsets at 2.85 K at 0 T, leading to a sharp peak in the temperature dependence of C/T , which is gradually suppressed by a transverse magnetic field [15]. By tracking the peak position in the field dependence of C/T , the critical field where the 3D magnetic order is fully suppressed was estimated to be $\mu_0 H_c^{\text{Co}} \sim 5.24$ T (μ_0 being the vacuum permeability) [15]. The most prominent feature of the specific heat data is the low-temperature plateau in C/T for fields slightly below H_c^{Co} , as exemplified by the 5 T data in Fig. 2(a). Such a plateau in C/T , i.e., a linear term in C is characteristic of gapless fermionic excitations. In an insulator like CoNb_2O_6 , such excitations are presumably from the magnetic degrees of freedom. These excitations constitute a large portion ($\sim 30\%$) of the total spin density of states [15], as evident by the larger value of both the low-temperature C/T [Figs. 2(a) and 2(b)] and magnetic entropy S_m [inset of Fig. 2(b)] at fields around H_c^{Co} than at lower and higher fields.

The thermal conductivity of an insulating magnet can generally be decomposed as $\kappa = \kappa_m + \kappa_p$, in which the two terms represent the contribution from magnetic excitations and phonons, respectively. If the magnetic excitations are gapless and fermionic, then in the simplest case (free fermions), they are expected to give rise to a linear contribution to κ , i.e., $\kappa_m \sim T$ [53]. At low temperatures ($T < 1$ K), phonons are usually scattered solely by the sample boundaries, so that $\kappa_p \sim T^\alpha$, where α is usually between 2 and 3 [53–55]. Combining these two

terms, one can fit the data to

$$\kappa/T = a + bT^{\alpha-1}, \quad (1)$$

and obtain a nonzero residual linear term $\kappa_0/T \equiv \kappa_m/T$ ($T \rightarrow 0$) = a from the gapless fermionic magnetic excitations, provided they are itinerant. Note that in some exotic cases, the magnetic excitations are not well-defined Landau quasiparticles—as exemplified by spinons in the presence of gauge fluctuations, and their thermal conductivity is expected to be sublinear and, again, one would get a finite κ_0/T when Eq. 1 is adopted [56, 57]. Therefore, one would expect (i) κ to be enhanced in the same field range where C is enhanced, and (ii) finite values of κ_0/T in this field range.

However, as shown in Figs. 2(c) and 2(d), neither feature was observed in our thermal conductivity data. In fact, κ shows an exactly opposite evolution with field as compared to C : κ is seen to be reduced at field values where C is enhanced. This is better visualized in Figs. 2(e) and 2(f), where $\Delta\kappa \equiv \kappa(H) - \kappa(0 \text{ T})$, and the field evolution of the normalized value of specific heat and thermal conductivity, are plotted, respectively. The fitting to Eq. 1 yields $a = -0.01 \pm 0.02 \text{ mW K}^{-2} \text{ cm}^{-1}$ and $\alpha = 2.45 \pm 0.04$ for 0 T, and $a = -0.44 \pm 0.05 \text{ mW K}^{-2} \text{ cm}^{-1}$ and $\alpha = 1.43 \pm 0.03$ for 5 T. At 0 T, the only candidate for heat carriers is the phonons. Indeed, κ_0/T is essentially negligible, and the value of α is consistent with the boundary scattering mechanism for phonons. At 5 T where the contribution to C from gapless magnetic excitations is most pronounced, the fitting

of κ gives, surprisingly, an unphysical negative κ_0/T and an α considerably smaller than the 0 T value and abnormally lower than 2.

The absence of a positive κ_0/T clearly rules out the direct contribution to κ from the gapless fermionic magnetic excitations around the QCP (see Sec. I in the Supplemental Material [58] for more discussions). This apparent contradiction with the specific heat data can only be removed if these excitations are localized. However, these excitations do have a substantial impact on κ : the value of κ and α should not change with magnetic field if the heat-carrying phonons are scattered solely by the sample boundary. The considerably smaller value of κ and the unusual value of α around H_c^{Co} signal the presence of other scattering mechanisms for phonons, with a scattering strength peaking in this field range. These features strongly suggest the additional scattering of phonons by the gapless magnetic excitations. As demonstrated in detail in Ref. [45], both the unphysical negative κ_0/T and the unusual values of α are consequences of forcing the fitting with Eq. 1 in systems with heat-carrying phonons scattered by magnetic degrees of freedom. At 5 T, which is slightly below the critical field, $\Delta\kappa$ is finite in almost the entire temperature range [Fig. 2(e)], consistent with the magnetic excitations that scatter phonons being gapless.

A natural speculation is that the localization of the magnetic excitations is induced by disorder. Localization effects in 1D systems have been investigated mainly in the charge sector [59], with only a few studies on the magnetic thermal conductivity for several spin ladder and spin chain systems [30–32, 60]. In the spin ladder compound $(\text{C}_5\text{H}_{12}\text{N})_2\text{CuBr}_4$, the absence of a measurable magnetic thermal conductivity was argued to result from spinon localization within finite ladder segments [32]. The thermal conductivity is thus dominated by the phonon contribution, which is scattered by the localized spinons via umklapp scattering [32]. This may seem to be a viable scenario for CoNb_2O_6 . However, this scenario is favored by the extremely weak interladder coupling of $(\text{C}_5\text{H}_{12}\text{N})_2\text{CuBr}_4$ (~ 27 mK). When the degree of one dimensionality is lowered, as in, e.g., the spin chain system $\text{Cu}(\text{C}_4\text{H}_4\text{N}_2)(\text{NO}_3)_2$, a similar scattering of phonons by localized magnetic excitations was proposed [30]. However, instead of tunneling through the strong impurities that cut the chains into segments, the excitations can now bypass the impurities by hopping to the neighbouring chains [30]. This leads to a considerable mean free path of the excitations and consequently a finite magnetic thermal conductivity [30]: the mean free path reaches ~ 750 μm in the spin chain system $\text{Ni}(\text{C}_2\text{H}_8\text{N}_2)_2\text{NO}_2(\text{ClO}_4)$, rendering the quasiparticle motion effectively 3D [31]. If at play, such hopping-assisted propagation of the magnetic excitations is expected to give rise to a measurable magnetic thermal conductivity in CoNb_2O_6 , a system much more 3D than the above-mentioned organic compounds, as reflected by its orders of magnitude larger interchain coupling

and transition temperatures of the 3D magnetic ordering [8, 9, 46, 61–63]. This is in sharp contrast to our observation (see Sec. I in the Supplemental Material [58] for an estimation of the mean free path).

Therefore, the localization mechanism of the magnetic excitations in CoNb_2O_6 must be distinct from the typical disorder-induced scenario in 1D spin systems, implying the essential role of the 3D nature and the consequent frustration. In fact, a similar picture of heat-carrying phonons scattered by localized magnetic degrees of freedom, has also been discussed for several famous quantum spin liquid candidates like YbMgGaO_4 [35], $\alpha\text{-RuCl}_3$ [38, 41], $\text{EtMe}_3\text{Sb}[\text{Pd}(\text{dmit})_2]_2$ [39, 40], and $\text{ZnCu}_3(\text{OH})_6\text{Cl}_2$ [45], as a consequence of the combination of disorder and frustration. From an experimental perspective, our finding of the localized nature of the critical excitations, together with the Kitaev physics unveiled by THz spectroscopy, and the glassy response found in a.c. calorimetry away from the QCP [15], highlights the complexity introduced by frustration to the physics of CoNb_2O_6 .

The origin of the fermionic excitations in the ordered phase as found by specific heat measurements is unclear [15]. One possibility is the quasiparticles arising from breaking the bound pairs of kinks [10]. In Ref. [15], however, it was argued that the magnetic excitations evident in specific heat should be entirely distinct from those observed by spectroscopy, considering the higher energy scale of the latter: the lowest discrete mode was observed around 1.2 meV at 0 T and 0.4 meV at 5 T, while the plateau in specific heat was observed below 1 K. Such an energy scale argument alone, however, does not necessarily exclude the possibility that the excitations seen in different probes share a similar origin. For an isolated Ising chain, the spectrum for critical kinks is gapless; however, in a quasi-1D magnet like CoNb_2O_6 , the nonzero interchain coupling can be approximated by an effective longitudinal field, which opens a gap and stabilizes the bound states, as observed in spectroscopy [7, 10, 14, 16, 64]. In this case, the gap is momentum dependent, leaving the gapless feature intact only at specific wave vectors [9]. In THz spectroscopy, the momentum space relevant to the optical responses is inherently limited to the Brillouin zone center. The neutron scattering measurements presented in Ref. [10] were performed in a scattering plane with an incomplete gap softening. Consequently, the critically soft magnetic spectrum may evade the detection of spectroscopic probes and manifest only in specific heat and thermal conductivity measurements, which treat all portions of the Brillouin zone on an equal footing.

A remaining issue is the field range associated with the critical excitations. Strictly speaking, closest agreement with the E8 mass ratio for the critical excitations is expected at the 1D QCP [64]. Although the gapless fermionic magnetic excitations were argued to be observed around the 3D QCP in Ref. [15], the distinction is not clear considering the closeness between the 1D and the 3D QCP in CoNb_2O_6 [10, 11, 15]. In this re-

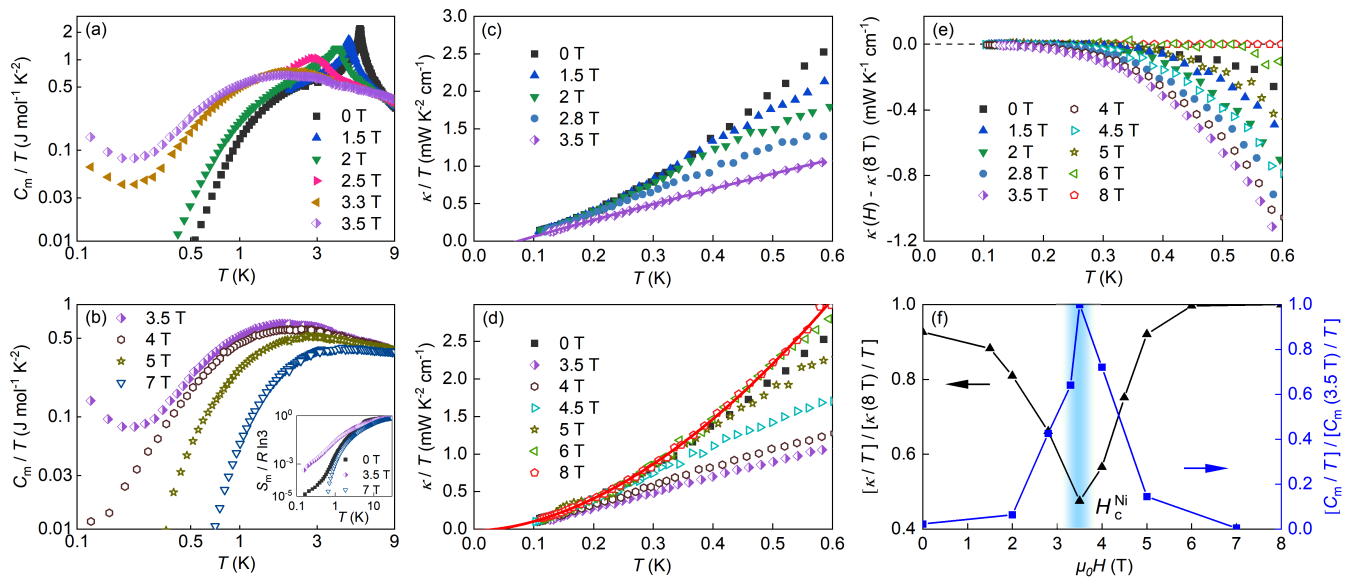


FIG. 3. (a,b) The magnetic specific heat C_m/T of NiNb_2O_6 below and above $\mu_0 H_c^{\text{Ni}} \sim 3.5$ T, respectively. The inset of (b) shows the magnetic entropy S_m of NiNb_2O_6 at selected fields. (c,d) The thermal conductivity κ/T of NiNb_2O_6 at fields below and above H_c^{Ni} , respectively. The solid lines are the fitting of the 3.5 and 8 T data to $\kappa/T = a + bT^{\alpha-1}$. (e) The influence of magnetic excitations on the thermal conductivity reflected in $\Delta\kappa \equiv \kappa(H) - \kappa(8 \text{ T})$. (f) The magnetic field evolution of the normalized thermal conductivity and magnetic specific heat at 0.4 K. The cyan shaded region depicts the position of H_c^{Ni} .

gard, it would be interesting to study the E8 excitations by specific heat and thermal conductivity measurements in $\text{BaCo}_2\text{V}_2\text{O}_8$, in which the 1D and 3D QCPs are well separated [65, 66].

The above discussion about the energy and field scales lead to the inference that it is likely that in CoNb_2O_6 , the magnetic excitations probed by various experimental probes are closely related, and the localized nature of these excitations revealed by our thermal conductivity data may have profound implications on all these previous studies.

B. Magnetic excitations around the QCP in NiNb_2O_6

The magnetic specific heat C_m of NiNb_2O_6 under various magnetic fields, obtained by subtracting the phonon specific heat estimated from the nonmagnetic counterpart ZnNb_2O_6 [67], is shown in Figs. 3(a) and 3(b). At 0 T, a clear peak marks the Néel temperature $T_N \sim 5.5$ K. With increasing field, the peak height is reduced and the peak is shifted to lower temperatures. We estimate the critical field where T_N is suppressed to zero as $\mu_0 H_c^{\text{Ni}} \sim 3.5$ T. Similar to CoNb_2O_6 , around H_c^{Ni} , C_m is significantly larger than that at lower and higher fields. Consequently, S_m [inset of Fig. 3(b)] at H_c^{Ni} is also seen to be larger than that at any other fields up to 5 K.

Moreover, at 3.3 and 3.5 T, C_m/T exhibits an upturn at the lowest temperatures, reminiscent of a Schottky contribution from nuclear spins. However, nuclear Schot-

tky contribution is expected to increase monotonically with field, inconsistent with our data. The upturn in C_m/T may eventually level off and form a plateau below the lowest temperature measured, similar to CoNb_2O_6 . Alternatively, it is also possible that the divergence is intrinsic. In either case, the critical-like divergent behavior of C_m/T signals the presence of magnetic degrees of freedom whose gap vanishes around the QCP.

Figures 3(c) and 3(d) show κ/T of NiNb_2O_6 at various fields along the a axis. The results with fields along b are similar, as shown in Sec. II in the Supplemental Material [58]. Similar to CoNb_2O_6 , κ/T is suppressed for field values around H_c^{Ni} , which is better illustrated in Fig. 3(e), where $\Delta\kappa \equiv \kappa(H) - \kappa(8 \text{ T})$ is plotted, and Fig. 3(f), where the field evolution of κ and C_m is displayed. Again, as a function of magnetic field, κ shows an anti-correlation with C_m , *i.e.*, κ is suppressed whenever C_m is enhanced. This immediately indicates that the magnetic degrees of freedom underlying C_m do not give a direct net contribution to κ , but serve as scattering centers for heat-carrying phonons instead. Indeed, the fitting to Eq. 1 yields $a = -0.01 \pm 0.01 \text{ mW K}^{-2} \text{ cm}^{-1}$ and $\alpha = 2.80 \pm 0.02$ for 8 T, and $a = -0.19 \pm 0.02 \text{ mW K}^{-2} \text{ cm}^{-1}$ and $\alpha = 1.91 \pm 0.02$ for 3.5 T. $\kappa(3.5 \text{ T})$ is suppressed relative to $\kappa(8 \text{ T})$ in the whole temperature range of our measurement, consistent with the gapless behavior seen in $C_m(3.5 \text{ T})$. Note also the lower value of $\kappa(0 \text{ T})$ than $\kappa(6 \text{ T})$ and $\kappa(8 \text{ T})$ (the latter two almost overlap), indicating the incomplete recovery of the phonon thermal conductivity for the former, which justifies our choice of $\kappa(8 \text{ T})$ as the reference data in the definition of $\Delta\kappa$.

To our knowledge, a similar divergent specific heat that only becomes evident at $T < \sim 0.3$ K with no concomitant thermal conductivity contribution was also observed in, e.g., the spin-triplet superconductor UTe₂, where it was attributed to a well-localized density of states or fermionic carriers that are heavily scattered [68].

C. Similarities between the phenomenology of CoNb₂O₆ and NiNb₂O₆

The similar set of phenomenology in CoNb₂O₆ and NiNb₂O₆, i.e., (i) an anticorrelation between the specific heat and thermal conductivity, with the former enhanced and the latter suppressed around the QCP, and (ii) an absence of the residual linear term and the unusual temperature scaling of the phonon thermal conductivity, point to a unified picture featuring localized critical magnetic excitations.

Although CoNb₂O₆ and NiNb₂O₆ share a similar structure, the similarities between the critical excitations are remarkable, considering the vast difference in their spin Hamiltonian. To obtain insights on a qualitative level, we consider here the simplest case of isolated chains. The spin Hamiltonian of CoNb₂O₆ under a transverse field is then:

$$H = -|J| \sum_{\langle i;j \rangle} S_i^z S_j^z - gH \sum_i S_i^x. \quad (2)$$

The spin Hamiltonian of NiNb₂O₆ under a transverse field can be described by:

$$H = -|J| \sum_{\langle i;j \rangle} \vec{S}_i \cdot \vec{S}_j - |D| \sum_i (S_i^z)^2 - gH \sum_i S_i^x. \quad (3)$$

Compared to Eq. 2, Eq. 3 features (a) spin-1 operators \vec{S}_i instead of spin-1/2, (b) a more isotropic exchange term $\vec{S}_i \cdot \vec{S}_j$, and (c) an additional term for the local on-site anisotropy D . While the TFIC model in Eq. 2 can be studied analytically, the Hamiltonian for NiNb₂O₆ has been studied numerically by exact diagonalization and density matrix renormalization group methods [52]. Some ‘in-between’ situations of these two distinct models, including the Blume-Capel model, which deal with (a) and (c) but with an Ising exchange term and without the coupling to external field, can also be rigorously solved [69–72]. In these models, compared to spin-1/2, the major consequence of the spin-1 nature is the existence of $S_z = 0$ states called holes. The holes separate the system into many independent segments of interacting $S = 1/2$ spins. The interplay between the hole excitations and the fermionic excitations within each spin-1/2

Ising segment hence determines the low temperature behavior and the quantum criticality [71, 72].

As discussed above, the physics of CoNb₂O₆ and NiNb₂O₆ goes well beyond the description of Eqs. 2 and 3, mainly as a result of the nonzero interchain coupling and the resultant frustration. The localized nature of the critical magnetic excitations in both compounds underscores the overarching role of the concerted effort of disorder and frustration in spin chain systems, and low dimensional magnets in a broader sense.

IV. SUMMARY

We measured the thermal conductivity of the Ising chain system CoNb₂O₆. We found an anticorrelation between the transverse field dependence of the thermal conductivity and that of the specific heat, the latter argued to be enhanced due to the quantum critical magnetic excitations which are gapless and fermionic. Contrary to the expectation that these excitations would contribute to a similar enhancement of the thermal conductivity, the heat current is solely carried by phonons which, however, are strongly scattered by the magnetic excitations. We argue that various experimental probes likely measure quantum critical excitations of a common origin, whose localized nature is unveiled for the first time by our thermal conductivity measurements. A similar set of phenomenology was also found in the spin-1 chain NiNb₂O₆, which likewise undergoes quantum transitions under a transverse field. The loss of mobility of the quantum critical excitations in two systems with magnetic properties distinct in many aspects, highlights a role of frustration not inferior to quantum criticality itself in spin chain systems.

ACKNOWLEDGEMENTS

We thank Y. Chen, Y. Zhou and J. D. Wu for helpful discussions. This work was supported by the Natural Science Foundation of China (Grant No. 12034004), the Ministry of Science and Technology of China (Grant No. 2016YFA0300503), and the Shanghai Municipal Science and Technology Major Project (Grant No. 2019SHZDZX01). Y. Xu was sponsored by the Shanghai Pujiang Program (Grant No: 21PJ1403100) and the Natural Science Foundation of Shanghai (Grant Nos: 21JC1402300 and 21ZR1420500). Work at the Johns Hopkins University was supported as part of the Institute for Quantum Matter, an EFRC funded by the DOE BES under DE-SC0019331.

L. S. Wang and Y. Xu contributed equally to this work.

[1] T. Senthil and M. P. A. Fisher, Z_2 gauge theory of electron fractionalization in strongly correlated systems,

- [2] T. Senthil and M. P. A. Fisher, Fractionalization in the cuprates: Detecting the topological order, *Phys. Rev. Lett.* **86**, 292 (2001).
- [3] F. D. M. Haldane, Nonlinear field theory of large-spin Heisenberg antiferromagnets: Semiclassically quantized solitons of the one-dimensional easy-axis Néel state, *Phys. Rev. Lett.* **50**, 1153 (1983).
- [4] T. Senthil, Symmetry-protected topological phases of quantum matter, *Annu. Rev. Condens. Matter Phys.* **6**, 299 (2015).
- [5] E. Lieb, T. Schultz, and D. Mattis, Two soluble models of an antiferromagnetic chain, *Ann. Phys. (N. Y.)* **16**, 407 (1961).
- [6] P. Pfeuty, The one-dimensional Ising model with a transverse field, *Ann. Phys. (N. Y.)* **57**, 79 (1970).
- [7] A. B. Zamolodchikov, Integrals of motion and S -matrix of the (scaled) $T = T_c$ Ising model with magnetic field, *Int. J. Mod. Phys. A* **04**, 4235 (1989).
- [8] S. Kobayashi, S. Mitsuda, M. Ishikawa, K. Miyatani, and K. Kohn, Three-dimensional magnetic ordering in the quasi-one-dimensional Ising magnet CoNb_2O_6 with partially released geometrical frustration, *Phys. Rev. B* **60**, 3331 (1999).
- [9] S. Lee, R. K. Kaul, and L. Balents, Interplay of quantum criticality and geometric frustration in columbite, *Nat. Phys.* **6**, 702 (2010).
- [10] R. Coldea, D. A. Tennant, E. M. Wheeler, E. Wawrzynska, D. Prabhakaran, M. Telling, K. Habicht, P. Smeibidl, and K. Kiefer, Quantum criticality in an Ising chain: Experimental evidence for emergent E8 symmetry, *Science* **327**, 177 (2010).
- [11] A. W. Kinross, M. Fu, T. J. Munsie, H. A. Dabkowska, G. M. Luke, S. Sachdev, and T. Imai, Evolution of quantum fluctuations near the quantum critical point of the transverse field Ising chain system CoNb_2O_6 , *Phys. Rev. X* **4**, 031008 (2014).
- [12] I. Cabrera, J. D. Thompson, R. Coldea, D. Prabhakaran, R. I. Bewley, T. Guidi, J. A. Rodriguez-Rivera, and C. Stock, Excitations in the quantum paramagnetic phase of the quasi-one-dimensional Ising magnet CoNb_2O_6 in a transverse field: Geometric frustration and quantum renormalization effects, *Phys. Rev. B* **90**, 014418 (2014).
- [13] N. J. Robinson, F. H. L. Essler, I. Cabrera, and R. Coldea, Quasiparticle breakdown in the quasi-one-dimensional Ising ferromagnet CoNb_2O_6 , *Phys. Rev. B* **90**, 174406 (2014).
- [14] C. M. Morris, R. Valdés Aguilar, A. Ghosh, S. M. Koohpayeh, J. Krizan, R. J. Cava, O. Tchernyshyov, T. M. McQueen, and N. P. Armitage, Hierarchy of bound states in the one-dimensional ferromagnetic Ising chain CoNb_2O_6 investigated by high-resolution time-domain terahertz spectroscopy, *Phys. Rev. Lett.* **112**, 137403 (2014).
- [15] T. Liang, S. M. Koohpayeh, J. W. Krizan, T. M. McQueen, R. J. Cava, and N. P. Ong, Heat capacity peak at the quantum critical point of the transverse Ising magnet CoNb_2O_6 , *Nat. Commun.* **6**, 7611 (2015).
- [16] K. Amelin, J. Engelmayer, J. Viirok, U. Nagel, T. Rõõm, T. Lorenz, and Z. Wang, Experimental observation of quantum many-body excitations of E_8 symmetry in the Ising chain ferromagnet CoNb_2O_6 , *Phys. Rev. B* **102**, 104431 (2020).
- [17] C. M. Morris, N. Desai, J. Viirok, D. Hübner, U. Nagel, T. Rõõm, J. W. Krizan, R. J. Cava, T. M. McQueen, S. M. Koohpayeh, R. K. Kaul, and N. P. Armitage, Duality and domain wall dynamics in a twisted Kitaev chain, *Nat. Phys.* **17**, 832 (2021).
- [18] S. Sachdev, *Quantum Phase Transitions*, 2nd ed. (Cambridge University Press, 2011).
- [19] W. Scharf, H. Weitzel, I. Yaeger, I. Maartense, and B. M. Wanklyn, Magnetic structures of CoNb_2O_6 , *J. Magn. Mater.* **13**, 121 (1979).
- [20] T. Hanawa, K. Shinkawa, M. Ishikawa, K. Miyatani, K. Saito, and K. Kohn, Anisotropic specific heat of CoNb_2O_6 in magnetic fields, *J. Phys. Soc. Jpn.* **63**, 2706 (1994).
- [21] G. H. Wannier, Antiferromagnetism. The triangular Ising net, *Phys. Rev.* **79**, 357 (1950).
- [22] Y. Wan and N. P. Armitage, Resolving continua of fractional excitations by spinon echo in THz 2D coherent spectroscopy, *Phys. Rev. Lett.* **122**, 257401 (2019).
- [23] J. Yang, W. Yuan, T. Imai, Q. Si, J. Wu, and M. Kormos, Local dynamics and thermal activation in the transverse-field Ising chain, [arXiv:2111.15107](https://arxiv.org/abs/2111.15107).
- [24] A. V. Sologubenko, K. Giannó, H. R. Ott, U. Ammerahl, and A. Revcolevschi, Thermal conductivity of the hole-doped spin ladder system $\text{Sr}_{14-x}\text{Ca}_x\text{Cu}_{24}\text{O}_{41}$, *Phys. Rev. Lett.* **84**, 2714 (2000).
- [25] A. V. Sologubenko, K. Giannò, H. R. Ott, A. Vietkine, and A. Revcolevschi, Heat transport by lattice and spin excitations in the spin-chain compounds SrCuO_2 and Sr_2CuO_3 , *Phys. Rev. B* **64**, 054412 (2001).
- [26] A. V. Sologubenko, H. R. Ott, G. Dhalenne, and A. Revcolevschi, Universal behavior of spin-mediated energy transport in $S=1/2$ chain cuprates: $\text{BaCu}_2\text{Si}_2\text{O}_7$ as an example, *EPL* **62**, 540 (2003).
- [27] C. Hess, C. Baumann, U. Ammerahl, B. Büchner, F. Heidrich-Meisner, W. Brenig, and A. Revcolevschi, Magnon heat transport in $(\text{Sr, Ca, La})_{14}\text{Cu}_{24}\text{O}_{41}$, *Phys. Rev. B* **64**, 184305 (2001).
- [28] C. Hess, B. Büchner, U. Ammerahl, L. Colonescu, F. Heidrich-Meisner, W. Brenig, and A. Revcolevschi, Magnon heat transport in doped La_2CuO_4 , *Phys. Rev. Lett.* **90**, 197002 (2003).
- [29] K. Kordonis, A. V. Sologubenko, T. Lorenz, S.-W. Cheong, and A. Freimuth, Spin thermal conductivity of the haldane chain compound Y_2BaNiO_5 , *Phys. Rev. Lett.* **97**, 115901 (2006).
- [30] A. V. Sologubenko, K. Berggold, T. Lorenz, A. Rosch, E. Shimshoni, M. D. Phillips, and M. M. Turnbull, Magnetothermal transport in the spin- $\frac{1}{2}$ chains of copper pyrazine dinitrate, *Phys. Rev. Lett.* **98**, 107201 (2007).
- [31] A. V. Sologubenko, T. Lorenz, J. A. Mydosh, A. Rosch, K. C. Shortsleeves, and M. M. Turnbull, Field-dependent thermal transport in the Haldane chain compound NENP, *Phys. Rev. Lett.* **100**, 137202 (2008).
- [32] A. V. Sologubenko, T. Lorenz, J. A. Mydosh, B. Thielemann, H. M. Rønnow, C. Rüegg, and K. W. Krämer, Evidence for spinon localization in the heat transport of the spin- $\frac{1}{2}$ ladder compound $(\text{C}_5\text{H}_{12}\text{N})_2\text{CuBr}_4$, *Phys. Rev. B* **80**, 220411 (2009).
- [33] M. Yamashita, N. Nakata, Y. Kasahara, T. Sasaki, N. Yoneyama, N. Kobayashi, S. Fujimoto, T. Shibauchi, and Y. Matsuda, Thermal-transport measurements in a quantum spin-liquid state of the frustrated triangular magnet κ -(BEDT-TTF) $_2\text{Cu}_2(\text{CN})_3$, *Nat. Phys.* **5**, 44 (2009).

- [34] M. Yamashita, N. Nakata, Y. Senshu, M. Nagata, H. M. Yamamoto, R. Kato, T. Shibauchi, and Y. Matsuda, Highly mobile gapless excitations in a two-dimensional candidate quantum spin liquid, *Science* **328**, 1246 (2010).
- [35] Y. Xu, J. Zhang, Y. S. Li, Y. J. Yu, X. C. Hong, Q. M. Zhang, and S. Y. Li, Absence of magnetic thermal conductivity in the quantum spin-liquid candidate YbMgGaO₄, *Phys. Rev. Lett.* **117**, 267202 (2016).
- [36] Y. J. Yu, Y. Xu, L. P. He, M. Kratochvilova, Y. Y. Huang, J. M. Ni, L. Wang, S.-W. Cheong, J.-G. Park, and S. Y. Li, Heat transport study of the spin liquid candidate 1T-TaS₂, *Phys. Rev. B* **96**, 081111 (2017).
- [37] I. A. Leahy, C. A. Pocs, P. E. Siegfried, D. Graf, S.-H. Do, K.-Y. Choi, B. Normand, and M. Lee, Anomalous thermal conductivity and magnetic torque response in the honeycomb magnet α -RuCl₃, *Phys. Rev. Lett.* **118**, 187203 (2017).
- [38] Y. J. Yu, Y. Xu, K. J. Ran, J. M. Ni, Y. Y. Huang, J. H. Wang, J. S. Wen, and S. Y. Li, Ultralow-temperature thermal conductivity of the Kitaev honeycomb magnet α -RuCl₃ across the field-induced phase transition, *Phys. Rev. Lett.* **120**, 067202 (2018).
- [39] J. M. Ni, B. L. Pan, B. Q. Song, Y. Y. Huang, J. Y. Zeng, Y. J. Yu, E. J. Cheng, L. S. Wang, D. Z. Dai, R. Kato, and S. Y. Li, Absence of magnetic thermal conductivity in the quantum spin liquid candidate EtMe₃Sb[Pd(dmit)₂]₂, *Phys. Rev. Lett.* **123**, 247204 (2019).
- [40] P. Bourgeois-Hope, F. Laliberté, E. Lefrançois, G. Grisonnanche, S. R. de Cotret, R. Gordon, S. Kitou, H. Sawa, H. Cui, R. Kato, L. Taillefer, and N. Doiron-Leyraud, Thermal conductivity of the quantum spin liquid candidate EtMe₃Sb[Pd(dmit)₂]₂: No evidence of mobile gapless excitations, *Phys. Rev. X* **9**, 041051 (2019).
- [41] R. Hentrich, A. U. B. Wolter, X. Zotos, W. Brenig, D. Nowak, A. Isaeva, T. Doert, A. Banerjee, P. Lampen-Kelley, D. G. Mandrus, S. E. Nagler, J. Sears, Y.-J. Kim, B. Büchner, and C. Hess, Unusual phonon heat transport in α -RuCl₃: Strong spin-phonon scattering and field-induced spin gap, *Phys. Rev. Lett.* **120**, 117204 (2018).
- [42] N. Li, Q. Huang, X. Y. Yue, W. J. Chu, Q. Chen, E. S. Choi, X. Zhao, H. D. Zhou, and X. F. Sun, Possible itinerant excitations and quantum spin state transitions in the effective spin-1/2 triangular-lattice antiferromagnet Na₂BaCo(PO₄)₂, *Nat. Commun.* **11**, 4216 (2020).
- [43] B. L. Pan, J. M. Ni, L. P. He, Y. J. Yu, Y. Xu, and S. Y. Li, Specific heat and thermal conductivity of the triangular-lattice rare-earth material KBaYb(BO₃)₂ at ultralow temperature, *Phys. Rev. B* **103**, 104412 (2021).
- [44] X. Rao, G. Hussain, Q. Huang, W. J. Chu, N. Li, X. Zhao, Z. Dun, E. S. Choi, T. Asaba, L. Chen, L. Li, X. Y. Yue, N. N. Wang, J.-G. Cheng, Y. H. Gao, Y. Shen, J. Zhao, G. Chen, H. D. Zhou, and X. F. Sun, Survival of itinerant excitations and quantum spin state transitions in YbMgGaO₄ with chemical disorder, *Nat. Commun.* **12**, 4949 (2021).
- [45] Y. Y. Huang, Y. Xu, L. Wang, C. C. Zhao, C. P. Tu, J. M. Ni, L. S. Wang, B. L. Pan, Y. Fu, Z. Hao, C. Liu, J.-W. Mei, and S. Y. Li, Heat transport in Herbertsmithite: Can a quantum spin liquid survive disorder?, [arXiv:2105.14749](https://arxiv.org/abs/2105.14749), accepted by Physical Review Letters.
- [46] C. Heid, H. Weitzel, P. Burlet, M. Bonnet, W. Gonschorek, T. Vogt, J. Norwig, and H. Fuess, Magnetic phase diagram of CoNb₂O₆: A neutron diffraction study, *J. Magn. Magn. Mater.* **151**, 123 (1995).
- [47] I. Yaeger, A. H. Morrish, and B. M. Wanklyn, Magnetization studies in transition-metal niobates: I. NiNb₂O₆, *Phys. Rev. B* **15**, 1465 (1977).
- [48] H. Liu and G. Khaliullin, Pseudospin exchange interactions in d^7 cobalt compounds: Possible realization of the Kitaev model, *Phys. Rev. B* **97**, 014407 (2018).
- [49] R. Sano, Y. Kato, and Y. Motome, Kitaev-Heisenberg Hamiltonian for high-spin d^7 Mott insulators, *Phys. Rev. B* **97**, 014408 (2018).
- [50] H. Liu, J. Chaloupka, and G. Khaliullin, Kitaev spin liquid in 3d transition metal compounds, *Phys. Rev. Lett.* **125**, 047201 (2020).
- [51] C. Heid, H. Weitzel, F. Bourdarot, R. Calemczuk, T. Vogt, and H. Fuess, Magnetism in FeNb₂O₆ and NiNb₂O₆, *J. Phys.: Condens. Matter* **8**, 10609 (1996).
- [52] P. Chauhan, F. Mahmood, H. J. Changlani, S. M. Koohpayeh, and N. P. Armitage, Tunable magnon interactions in a ferromagnetic spin-1 chain, *Phys. Rev. Lett.* **124**, 037203 (2020).
- [53] J. M. Ziman, *Electrons and Phonons: The Theory of Transport Phenomena in Solids* (Oxford University Press, Oxford, 1963).
- [54] M. Sutherland, D. G. Hawthorn, R. W. Hill, F. Ronning, S. Wakimoto, H. Zhang, C. Proust, E. Boaknin, C. Lupien, L. Taillefer, R. Liang, D. A. Bonn, W. N. Hardy, R. Gagnon, N. E. Hussey, T. Kimura, M. Nohara, and H. Takagi, Thermal conductivity across the phase diagram of cuprates: Low-energy quasiparticles and doping dependence of the superconducting gap, *Phys. Rev. B* **67**, 174520 (2003).
- [55] S. Y. Li, L. Taillefer, C. H. Wang, and X. H. Chen, Ballistic magnon transport and phonon scattering in the antiferromagnet Nd₂CuO₄, *Phys. Rev. Lett.* **95**, 156603 (2005).
- [56] S.-S. Lee and P. A. Lee, U(1) gauge theory of the Hubbard Model: Spin liquid states and possible application to κ -(BEDT-TTF)₂Cu₂(CN)₃, *Phys. Rev. Lett.* **95**, 036403 (2005).
- [57] C. P. Nave and P. A. Lee, Transport properties of a spinon Fermi surface coupled to a U(1) gauge field, *Phys. Rev. B* **76**, 235124 (2007).
- [58] See Supplemental Material for more discussions on the localized nature of the magnetic excitations, and the thermal conductivity of NiNb₂O₆ with the magnetic field along the b axis, which includes Refs. [10, 34, 39, 40, 46, 51, 52].
- [59] T. Giamarchi, *Quantum Physics in One Dimension* (Oxford University Press, 2004).
- [60] A. Karahalios, A. Metavitsiadis, X. Zotos, A. Gorczyca, and P. Prelovšek, Finite-temperature transport in disordered Heisenberg chains, *Phys. Rev. B* **79**, 024425 (2009).
- [61] L. P. Regnault, I. Zaliznyak, J. P. Renard, and C. Vettier, Inelastic-neutron-scattering study of the spin dynamics in the Haldane-gap system Ni(C₂H₈N₂)₂NO₂(ClO₄), *Phys. Rev. B* **50**, 9174 (1994).
- [62] T. Lancaster, S. J. Blundell, M. L. Brooks, P. J. Baker, F. L. Pratt, J. L. Manson, C. P. Landee, and C. Baines, Magnetic order in the quasi-one-dimensional spin-1/2 molecular chain compound copper pyrazine dinitrate, *Phys. Rev. B* **73**, 020410 (2006).
- [63] M. Klanjšek, H. Mayaffre, C. Berthier, M. Horvatić, B. Chiari, O. Piovesana, P. Bouillot, C. Kollath, E. Orignac, R. Citro, and T. Giamarchi, Controlling Lut-

- tinger liquid physics in spin ladders under a magnetic field, *Phys. Rev. Lett.* **101**, 137207 (2008).
- [64] S. T. Carr and A. M. Tsvelik, Spectrum and correlation functions of a quasi-one-dimensional quantum Ising model, *Phys. Rev. Lett.* **90**, 177206 (2003).
- [65] Z. Zhang, K. Amelin, X. Wang, H. Zou, J. Yang, U. Nagel, T. R oom, T. Dey, A. A. Nugroho, T. Lorenz, J. Wu, and Z. Wang, Observation of E_8 particles in an Ising chain antiferromagnet, *Phys. Rev. B* **101**, 220411 (2020).
- [66] H. Zou, Y. Cui, X. Wang, Z. Zhang, J. Yang, G. Xu, A. Okutani, M. Hagiwara, M. Matsuda, G. Wang, G. Mussardo, K. H ods agi, M. Kormos, Z. He, S. Kimura, R. Yu, W. Yu, J. Ma, and J. Wu, E_8 spectra of quasi-one-dimensional antiferromagnet $\text{BaCo}_2\text{V}_2\text{O}_8$ under transverse field, *Phys. Rev. Lett.* **127**, 077201 (2021).
- [67] T. Hanawa, M. Ishikawa, and K. Miyatani, Disappearance of ferromagnetism at low temperatures in CoNb_2O_6 , *J. Phys. Soc. Jpn.* **61**, 4287 (1992).
- [68] T. Metz, S. Bae, S. Ran, I.-L. Liu, Y. S. Eo, W. T. Fuhrman, D. F. Agterberg, S. M. Anlage, N. P. Butch, and J. Paglione, Point-node gap structure of the spin-triplet superconductor UTe_2 , *Phys. Rev. B* **100**, 220504 (2019).
- [69] M. Blume, Theory of the first-order magnetic phase change in UO_2 , *Phys. Rev.* **141**, 517 (1966).
- [70] H. W. Capel, On the possibility of first-order phase transitions in Ising systems of triplet ions with zero-field splitting, *Physica (Amsterdam)* **32**, 966 (1966).
- [71] Z. Yang, L. Yang, J. Dai, and T. Xiang, Rigorous solution of the spin-1 quantum Ising model with single-ion anisotropy, *Phys. Rev. Lett.* **100**, 067203 (2008).
- [72] Z.-H. Yang, L.-P. Yang, H.-N. Wu, J. Dai, and T. Xiang, Exact solutions of a class of $S = 1$ quantum Ising spin models, *Phys. Rev. B* **79**, 214427 (2009).